



HAL
open science

Detection of protonated formaldehyde in the prestellar core L1689B

A. Bacmann, E. García-García, A. Faure

► **To cite this version:**

A. Bacmann, E. García-García, A. Faure. Detection of protonated formaldehyde in the prestellar core L1689B. *Astronomy and Astrophysics - A&A*, 2016, 588, 10.1051/0004-6361/201628280 . insu-03691558

HAL Id: insu-03691558

<https://insu.hal.science/insu-03691558>

Submitted on 9 Jun 2022

HAL is a multi-disciplinary open access archive for the deposit and dissemination of scientific research documents, whether they are published or not. The documents may come from teaching and research institutions in France or abroad, or from public or private research centers.

L'archive ouverte pluridisciplinaire **HAL**, est destinée au dépôt et à la diffusion de documents scientifiques de niveau recherche, publiés ou non, émanant des établissements d'enseignement et de recherche français ou étrangers, des laboratoires publics ou privés.

LETTER TO THE EDITOR

Detection of protonated formaldehyde in the prestellar core L1689B^{★,★★}

A. Bacmann^{1,2}, E. García-García^{1,2}, and A. Faure^{1,2}

¹ Univ. Grenoble Alpes, IPAG, 38000 Grenoble, France
e-mail: aureore.bacmann@univ-grenoble-alpes.fr

² CNRS, IPAG, 38000 Grenoble, France

Received 9 February 2016 / Accepted 29 February 2016

ABSTRACT

Complex organic molecules (COMs) are detected in many regions of the interstellar medium, including prestellar cores. However, their formation mechanisms in cold (~ 10 K) cores remain to this date poorly understood. The formyl radical HCO is an important candidate precursor for several O-bearing terrestrial COMs in cores, as an abundant building block of many of these molecules. Several chemical routes have been proposed to account for its formation: on grain surfaces, as an incompletely hydrogenated product of H addition to frozen-out CO molecules; and in the gas phase, either as the product of the reaction between H₂CO and a radical or as a product of dissociative recombination of protonated formaldehyde H₂COH⁺. The detection and abundance determination of H₂COH⁺, if present, could provide clues as to whether this latter scenario might apply. We searched for protonated formaldehyde H₂COH⁺ in the prestellar core L1689B using the IRAM 30 m telescope. The H₂COH⁺ ion is unambiguously detected, for the first time, in a cold (~ 10 K) source. The derived abundance agrees with a scenario in which the formation of H₂COH⁺ results from the protonation of formaldehyde. We use this abundance value to constrain the branching ratio of the dissociative recombination of H₂COH⁺ towards the HCO channel to ~ 10 –30%. This value could however be lower if HCO were efficiently formed from neutral-neutral reactions in the gas phase, and we stress the need for laboratory measurements of the rate constants of these reactions at 10 K. Given the experimental difficulties in measuring branching ratios experimentally, observations can place valuable constraints on these values and provide useful input for chemical networks.

Key words. ISM: molecules – line: identification – ISM: abundances

1. Introduction

Despite their low temperatures, prestellar cores harbour a wealth of chemical species. In recent years, complex organic molecules (COMs), which were previously thought to trace mainly warm gas in star-forming regions, have been detected in prestellar sources (e.g. Bacmann et al. 2012; Vastel et al. 2014) where the temperatures are around 10 K. The formation mechanisms of the terrestrial COMs, (i.e. which are stable under Earth-like conditions) currently detected in the cold gas remain poorly understood, and the respective roles of gas-phase reactions or grain surface chemistry are still being debated.

Radicals like the formyl radical HCO or the methoxy radical CH₃O have drawn attention as the possible precursors of COMs, either in the gas phase (Vasyunin & Herbst 2013; Balucani et al. 2015) or on grain surfaces (Garrod & Herbst 2006). They are also important intermediates in the grain-surface synthesis of methanol, as products of H-atom additions to CO (e.g. Brown et al. 1988; Pirim & Krim 2011). These radicals are also widely detected in the gas phase of prestellar cores and cold clouds (Bacmann & Faure 2016; Agúndez et al. 2015b; Gerin et al. 2009; Cernicharo et al. 2012).

In a previous survey of these radicals in a sample of prestellar cores, Bacmann & Faure (2016) proposed that the HCO abundances measured in the gas phase could be accounted for by a pure gas-phase scenario, in which HCO results from the dissociative recombination of protonated formaldehyde H₂COH⁺. In dark clouds, H₂COH⁺ is likely the product of the protonation of H₂CO, which is an abundant organic species in prestellar cores, with abundances generally around 10^{-10} – 10^{-9} (Bacmann et al. 2003; Guzmán et al. 2011). Proton donors, such as H₃⁺, or HCO⁺, are the most abundant ions, with abundances close to 10^{-9} – 10^{-8} (Aikawa et al. 2005; Flower et al. 2005, 2006). It is therefore expected that protonated formaldehyde H₂COH⁺ would easily be formed. Previous searches by Minh et al. (1993) towards Orion A and the two cold clouds L183 and TMC-1 yielded no detection, and Ohishi et al. (1996) detected H₂COH⁺ only towards Sgr B2 and several hot cores and not towards the cold sources of their sample.

In this Letter, we present the first detection of protonated formaldehyde in a cold core, and discuss its abundance in terms of the formation of the HCO radical by ion-molecule chemistry, and the possibility to constrain the branching ratio towards HCO of its dissociative recombination with electrons.

2. Observations and data analysis

The frequencies of the rotational transitions of H₂COH⁺ were determined by Chomiak et al. (1994) and Dore et al. (1995) and were retrieved from the CDMS spectroscopy catalogue (Müller et al. 2001, 2005). Line excitation is always an issue in cold (~ 10 K) gas and only levels with a low energy can be populated. To search for H₂COH⁺, we therefore selected transitions with

* Based on observations carried out with the IRAM 30 m telescope. IRAM is supported by INSU/CNRS (France), MPG (Germany), and IGN (Spain).

** Final IRAM data used in the paper (FITS cubes) are only available at the CDS via anonymous ftp to cdsarc.u-strasbg.fr (130.79.128.5) or via <http://cdsarc.u-strasbg.fr/viz-bin/qcat?J/A+A/588/L8>

Table 1. Observed H_2COH^+ transitions.

Transition $J_{K_a K_c}$	Frequency MHz	E_{up} K	g_{up}	A_{ul} s^{-1}
$4_{04}-3_{13}$	102 065.86	30.4	9	7.27×10^{-6}
$2_{02}-1_{11}$	126 923.38	9.1	5	1.83×10^{-5}
$2_{11}-1_{10}$	132 219.70	17.5	5	1.55×10^{-5}
$1_{10}-1_{01}$	168 401.14	11.1	3	8.77×10^{-5}

upper level energies lower than ~ 20 K, which could be observed in a minimum of frequency setups, and for which good atmospheric transmission did not require very dry weather conditions. The chosen three lines at 2 mm and their spectroscopic parameters are shown in Table 1, to which we added a line at 3 mm from a previous project.

The observations were carried out towards the prestellar core L1689B in January and March 2012 for the 3 mm transition and in March 2015 for the 2 mm transitions with the IRAM 30 m telescope located at Pico Veleta, Spain. The source was selected on the grounds that its molecular lines are usually stronger than in other similar sources (Bacmann & Faure 2016). The integration coordinates were $\alpha_{2000} = 16^{\text{h}}34^{\text{m}}48.30^{\text{s}}$ and $\delta_{2000} = -24^{\circ}38'04.0''$, corresponding to the peak of the millimetre dust continuum emission. We used the receivers E090 and E150 operating at 3 mm and 2 mm, respectively, which were connected to the Fourier transform spectrometer (FTS) at a frequency resolution of ~ 50 kHz; this corresponded to velocity resolutions of 0.15 km s^{-1} at 102 GHz, 0.11 km s^{-1} at 130 GHz, and 0.09 km s^{-1} at 170 GHz. The weather conditions were good during the 2012 observing runs, and excellent during the March 2015 run with precipitable water vapour of 1 mm on average and system temperatures of ~ 80 K at 126–132 GHz and ~ 130 K at 170 GHz. Pointing was checked every 1.5 h on a nearby quasar and found to be within $2-3''$ at 2 mm and $3-4''$ at 3 mm. Focus was performed on a strong quasar at the beginning of each observing session and on Mercury after sunrise. The data were taken with the frequency switching mode with a frequency throw of 7.5 MHz. The antenna forward efficiency F_{eff} is 0.95 and 0.93 at 3 mm and 2 mm, respectively, and the main beam efficiencies B_{eff} were taken to be 0.79, 0.77, 0.76, and 0.70 at 106.1 GHz, 126.9 GHz, 132.2 GHz, and 168.4 GHz, respectively. From integrations carried out at different offsets (which is discussed elsewhere), we find that the emission fills the main beam but is not very extended, and therefore we used the main beam temperature scale in our analysis, applying $T_{\text{mb}} = F_{\text{eff}}/B_{\text{eff}} T_{\text{a}}^*$. The main beam size is $24''$ at 106.1 GHz, $19''$ at 126.9 GHz and at 132.2 GHz, and $15''$ at 168.4 GHz.

The data were reduced using the IRAM GILDAS/CLASS¹ software: the individual scans were averaged together and a low-order (typically 3) polynomial was fitted to line-free regions of the spectra to subtract a baseline. The resulting spectra were then folded to recover from the effect of the frequency switching procedure.

3. Column density determination

Protonated formaldehyde is clearly detected, as can be seen from the spectra shown in Fig. 1. The transition at 102 GHz is however not detected, which can be explained by its lower Einstein spontaneous emission coefficient and higher upper level energy. The line parameters, velocity integrated intensities, line widths, and peak line intensities, were determined by fitting a Gaussian to each line. The obtained values are presented in Table 2.

¹ <http://www.iram.fr/IRAMFR/GILDAS>

Table 2. Line parameters for the observed H_2COH^+ transitions.

Frequency MHz	rms mK	T_{mb} mK	Δv km s^{-1}	Integrated intensity K km s^{-1}
102 065.86	3.3	–	–	<0.0024
126 923.38	6.0	116	0.45 (0.02)	0.0553 (0.0085)
132 219.70	2.6	12	0.35 (0.06)	0.0043 (0.0010)
168 401.14	7.6	67	0.40 (0.03)	0.0290 (0.0048)

Notes. The rms is given for 50 kHz channels. The numbers between parenthesis are the 1σ uncertainties. The upper limit is 3σ .

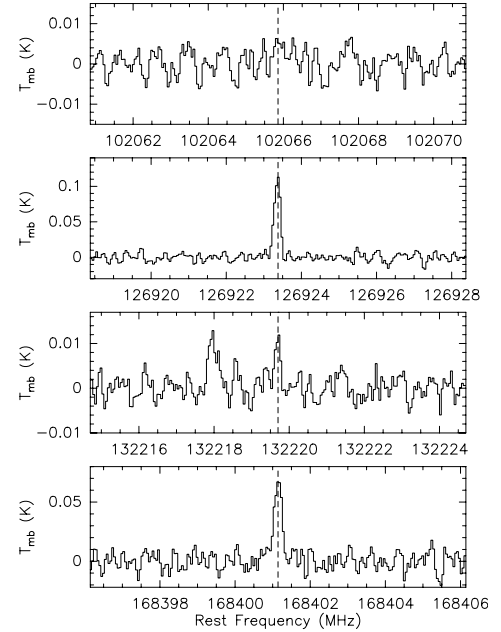


Fig. 1. H_2COH^+ spectra in L1689B. The vertical dashed lines indicate the positions of the H_2COH^+ transitions. The feature at ~ 132218 MHz does not correspond to any line from the CDMS or the JPL catalogue.

There are no available collisional coefficients for H_2COH^+ , so we perform a simple derivation of the column density assuming local thermodynamic equilibrium (LTE). The method we use has been described in Bacmann & Faure (2016). Briefly, we calculate the integrated intensities of the transitions under the LTE assumption for a range of column density and excitation temperature values, and perform a least-squares fit, defining a χ^2 between the calculated integrated intensities and observed integrated intensities for the detected lines.

The best model yields a column density of $6.7 \times 10^{11} \text{ cm}^{-2}$ and a temperature of 4.2 K. Reasonably good fits (i.e. for which χ^2 is within 1σ of the minimum χ^2 value) can be found for high values of the column density ($\geq 1.5 \times 10^{12} \text{ cm}^{-2}$), but these fits are obtained for excitation temperatures that are below 3.5 K. We limit ourselves to excitation temperatures above 3.7 K because lower values become unrealistic. With this additional condition, we find that the beam averaged H_2COH^+ column density is between $3.3 \times 10^{11} \text{ cm}^{-2}$ and $1.1 \times 10^{12} \text{ cm}^{-2}$. The non-detection of the 102 GHz line does not bring supplementary constraints despite the high sensitivity of the observation because the low excitation temperatures considered (< 5 K) are compatible with a non-detection of this line even for unrealistically high column densities, for which the other lines would be stronger and optically thick. Despite the low number of lines in our analysis, the best fit is only moderately good, as shown in Fig. 2. This probably means that the excitation deviates from LTE.

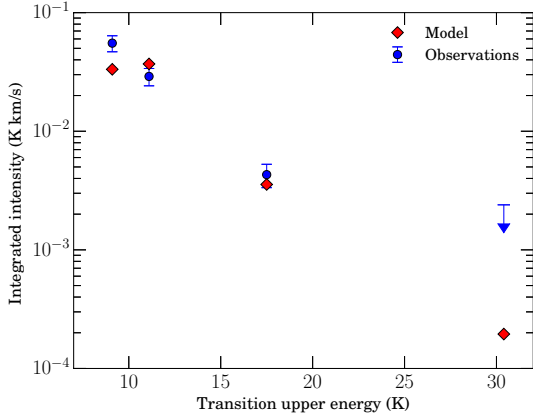
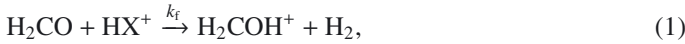


Fig. 2. Comparison of modelled and observed integrated intensities for the four considered H_2COH^+ transitions.

4. Discussion and conclusions

This detection represents the first detection of protonated formaldehyde in a cold prestellar core. Former searches for this ion in similar sources did not yield any detection, most probably because of lack of sensitivity in the observations. The spectral resolution of the H_2COH^+ non-detections in the cold sources of [Ohishi et al. \(1996\)](#) is ambiguous. If we assume that it was 250 kHz, the rms noise of 20 mK reached by [Ohishi et al. \(1996\)](#) was not low enough to detect the 168.4 GHz line if it was as strong as in L1689B.

Most likely, the dominant reaction route to form H_2COH^+ in dark clouds is the protonation of formaldehyde



where HX^+ stands for a proton donor. Indeed, both H_2CO and proton donors (e.g. H_3^+ , its deuterated isotopologues, or HCO^+) are abundant in prestellar cores, and exothermic ion-molecule processes are generally fast. [Bacmann & Faure \(2016\)](#) estimated the rate for reaction (1) with $\text{HX}^+ = \text{H}_3^+$ to be $k_f = 7 \times 10^{-8} \text{ cm}^3 \text{ s}^{-1}$ at 10 K, using the locked dipole approximation. Because of the difference in reduced mass, this rate constant becomes $k_f = 3.1 \times 10^{-8} \text{ cm}^3 \text{ s}^{-1}$ at 10 K if $\text{HX}^+ = \text{HCO}^+$. The most efficient destruction route for H_2COH^+ is the dissociative recombination (DR) with electrons



Reaction (2) was studied experimentally by [Hamberg et al. \(2007\)](#), and recently by [Osborne et al. 2015](#)) who determined $k_d = 9.9 \times 10^{-6} \text{ cm}^3 \text{ s}^{-1}$ at 10 K. At steady state, if H_2COH^+ is indeed formed mostly by reaction (1) and destroyed by reaction (2), its abundance is simply given by

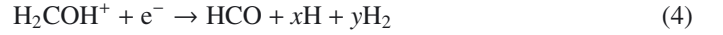
$$[\text{H}_2\text{COH}^+] = \frac{k_f}{k_d} \frac{[\text{HX}^+]}{[\text{e}^-]} [\text{H}_2\text{CO}]. \quad (3)$$

Substituting the reaction rates with their values for H_3^+ and assuming the proton donor abundance is equal to the electron abundance, we predict an abundance of $[\text{H}_2\text{COH}^+] \approx 0.007 [\text{H}_2\text{CO}]$ as mentioned in [Bacmann & Faure \(2016\)](#), or $[\text{H}_2\text{COH}^+] \approx 0.003 [\text{H}_2\text{CO}]$ if HCO^+ is the main proton donor. Using an H_2CO column density of $1.3 \times 10^{14} \text{ cm}^{-2}$ ([Bacmann et al. 2003](#)), we find that the predicted H_2COH^+ column density N^{mod} derived from Eq. (3) is $4.1 \times 10^{11} - 9.1 \times 10^{11} \text{ cm}^{-2}$ (depending on the main proton donor), which is consistent with the

observed value we determine in L1689B, $N^{\text{obs}} = 6.7 \times 10^{11} \text{ cm}^{-2}$ within the uncertainties. This also nicely confirms the value of the destruction rate of H_2COH^+ measured by [Hamberg et al. \(2007\)](#) at 10 K.

[Agúndez et al. \(2015a\)](#) have run a time-dependent chemical model using the UMIST12 network ([McElroy et al. 2013](#)) and derive $[\text{H}_2\text{COH}^+] \sim 8 \times 10^{-4} - 10^{-3} [\text{H}_2\text{CO}]$, about six times smaller than our observed value. Though our model better reproduces the observations, it considers only one formation and one destruction route for H_2COH^+ . The H_2CO protonation reactions in the UMIST12 network producing H_2COH^+ have smaller reaction rates than the rate we use (a factor of 2). Our model might also overestimate the amount of proton donors reacting with H_2CO , since we assume it equal to the electron abundance. We also neglect other destruction routes than electronic DR for H_2COH^+ , such as proton transfer between H_2COH^+ and CH_3OH or NH_3 , but these are about 1000 times slower than DR at 10 K and unlikely to be a cause for the discrepancy between both models.

The dissociative recombination of H_2COH^+ with electrons has several output channels. According to the experiments by [Hamberg et al. \(2007\)](#), the products of the reaction are



where x and y are integers that account for the different possible combinations of H and H_2 in the products. The experimental branching ratios are 6% for CH_2 , 2% for CH , and 92% for the channels where the C–O bond is conserved (i.e. CO , HCO , and H_2CO). This is in contrast to the dissociative recombination of CH_3OH for which the C–O bond is preserved in a minority of channels ([Geppert et al. 2006](#)). In the case of H_2COH^+ , the experiment by [Hamberg et al. \(2007\)](#) did not distinguish between HCO , CO , and H_2CO .

In order to account for the gas-phase abundance of the HCO radical in a sample of prestellar cores, and in particular the constant abundance ratio of ~ 10 between H_2CO and HCO , [Bacmann & Faure \(2016\)](#) suggested that the observed $\text{HCO}/\text{H}_2\text{CO}$ abundance ratio can be reproduced if HCO originates from the dissociative recombination of H_2COH^+ , assuming that the branching ratio of the DR is $\sim 10\%$ for the HCO channel (reaction (4) above). Although the detection of H_2COH^+ in a prestellar core does not provide unambiguous evidence that HCO forms from the protonation of formaldehyde followed by dissociative recombination, it is still in agreement with this scenario, and allows us to directly constrain the branching ratio of the dissociative recombination for the HCO channel. In this framework, and assuming the main destruction route for HCO is with a proton donor like H_3^+ , the branching ratio f for HCO is given by

$$k_{\text{dd}} [\text{HCO}][\text{H}_3^+] = f k_d [\text{H}_2\text{COH}^+][\text{e}^-],$$

where $k_{\text{dd}} = 5 \times 10^{-8} \text{ cm}^3 \text{ s}^{-1}$ is the destruction rate of HCO with H_3^+ at 10 K ([Bacmann & Faure 2016](#)). Assuming as before $[\text{H}_3^+] \approx [\text{e}^-]$, the H_2COH^+ column density determined in this study ($N_{\text{H}_2\text{COH}^+}^{\text{obs}} = 6.7 \times 10^{11} \text{ cm}^{-2}$) and the HCO column density in L1689B given in [Bacmann & Faure \(2016\)](#) ($N_{\text{HCO}} = 1.3 \times 10^{13} \text{ cm}^{-2}$), we find again $f \sim 10\%$, without invoking the H_2CO abundance.

As discussed in [Bacmann & Faure \(2016\)](#), another potential destruction route for HCO is with abundant atoms such as H. In this case, assuming an atomic H abundance of $\sim 10^{-5}$ with respect to H₂, an electronic abundance of 10^{-8} , and $k_{\text{H}} = 1.5 \times 10^{-10} \text{ cm}^3 \text{ s}^{-1}$ for the rate constant of the reaction HCO + H (the value at 300 K from [Baulch et al. 2005](#)), we find a value for the branching ratio f of 30%. It is however unclear whether the value of k_{H} taken here also applies at 10 K, since no measurements of this rate constant are available at low temperatures.

One major uncertainty in this determination of the branching ratio results from possible alternative formation scenarios for HCO, which could be non-negligible. One such route is the neutral-neutral reaction between H₂CO and an abundant radical such as OH or CN. Recent experimental studies have confirmed that such reactions could proceed efficiently via tunnelling at low temperatures. Indeed, [Shannon et al. \(2013\)](#) and [Gómez Martín et al. \(2014\)](#) have shown that the reaction CH₃OH + OH gets faster at low temperatures down to ~ 50 K. A spectacular increase in the reaction constant is also reported by [Jiménez et al. \(2016\)](#) for CH₃OCHO + OH; the reaction rate increases by three orders of magnitude between 300 K and 22 K and by an order of magnitude between 60 K and 22 K, reaching as high a value as $1.2 \times 10^{-10} \text{ cm}^3 \text{ s}^{-1}$. In order to be as efficient as the ion-molecule route to form HCO, the constant of the reaction between H₂CO and OH would have to be $4 \times 10^{-10} \text{ cm}^3 \text{ s}^{-1}$ at 10 K ([Bacmann & Faure 2016](#)). No measurements at 10 K of this reaction, or of reactions similar to this, are available, but they are needed because the behaviour of the reaction constant is not known below 230 K (at which temperature it is $10^{-11} \text{ cm}^3 \text{ s}^{-1}$) and extrapolation is hazardous. In the case that H₂CO + OH would be a major formation channel for HCO, the observed HCO abundance could be accounted for without the need for the DR of H₂COH⁺ to yield a significant amount of HCO. In this respect, the branching ratio we determined above can be considered an upper limit².

This result can have implications for chemical networks because they assume statistical weights for the three products CO, HCO, and H₂CO (1/3, 1/3, 1/3), as in the UMIST12 network or the KIDA³ database ([Wakelam et al. 2012](#)), following [Prasad & Huntress \(1980\)](#). As already noted in [Hamberg et al. \(2007\)](#), these branching ratios are still vastly in agreement with their experimental results, which state that CO, HCO and H₂CO represent over 90% of the products. However, the branching ratio that is needed here to account for the observed HCO and H₂COH⁺ abundances could be significantly different from the statistical value, as it could be 10%, or lower.

This value should however be taken with some caution because the excitation of H₂COH⁺ is not constrained well in the absence of collisional coefficients. Our estimation of the branching ratio should therefore be repeated once collisional coefficients for H₂COH⁺ become available. Observations of H₂COH⁺ in other prestellar sources are also needed to confirm the current findings.

To conclude, we report the detection of protonated formaldehyde H₂COH⁺ in the prestellar source L1689B. The derived beam-averaged column density is $6.7 \times 10^{11} \text{ cm}^{-2}$, corresponding to an abundance of $\sim 1.9 \times 10^{-11}$ with respect to H₂, if we

² We also note that the neutral-neutral reaction CH₂ + O should yield negligible amounts of HCO in the conditions prevailing in cold cores (see KIDA datasheet on this reaction). Using the rate constant in the KIDA database ($2 \times 10^{-12} \text{ cm}^3 \text{ s}^{-1}$) and the steady-state abundances of CH₂ and O from the model of [Le Gal et al. \(2014\)](#), we find that this reaction is 100 times less efficient than the DR of H₂COH⁺ at forming HCO.

³ <http://kida.obs.u-bordeaux1.fr>

assume an H₂ column density of $3.6 \times 10^{22} \text{ cm}^{-2}$ ([Roy et al. 2014](#)). It is likely however that this abundance is overestimated, as the H₂ column density in [Roy et al. \(2014\)](#) is averaged over a 36'' beam and is probably higher in the 15–19'' beam of our H₂COH⁺ observations. The H₂COH⁺ column density agrees with the destruction rate of H₂COH⁺ by dissociative recombination as measured by [Hamberg et al. \(2007\)](#), supposing that H₂COH⁺ is mostly formed by protonation of H₂CO in prestellar cores and destroyed by electronic dissociative recombination. Using previous observations of the radical HCO in the same source, we constrain the branching ratio of H₂COH⁺ to HCO to be around 10–30% or lower if HCO is significantly formed by gas-phase reactions between H₂CO and a radical. The experimental determination of branching ratios is a fundamental piece of data in astrochemistry, but in case these measurements are not available, observations can place valuable constraints on the branching ratios, as demonstrated here.

Acknowledgements. This work has benefitted from the support of the CNRS programme “Physique et Chimie du Milieu Interstellaire” (PCMI). E. García-García acknowledges support from an Alpes Grenoble Innovation Recherche (AGIR) grant.

References

- Agúndez, M., Cernicharo, J., de Vicente, P., et al. 2015a, *A&A*, 579, L10
 Agúndez, M., Cernicharo, J., & Guélin, M. 2015b, *A&A*, 577, L5
 Aikawa, Y., Herbst, E., Roberts, H., & Caselli, P. 2005, *ApJ*, 620, 330
 Bacmann, A., & Faure, A. 2016, *A&A*, 587, A130
 Bacmann, A., Lefloch, B., Ceccarelli, C., et al. 2003, *ApJ*, 585, L55
 Bacmann, A., Taquet, V., Faure, A., Kahane, C., & Ceccarelli, C. 2012, *A&A*, 541, L12
 Balucani, N., Ceccarelli, C., & Taquet, V. 2015, *MNRAS*, 449, L16
 Baulch, D. L., Bowman, C. T., Cobos, C. J., et al. 2005, *J. Phys. Chem. Ref. Data*, 34, 757
 Brown, P. D., Charnley, S. B., & Millar, T. J. 1988, *MNRAS*, 231, 409
 Cernicharo, J., Marcelino, N., Roueff, E., et al. 2012, *ApJ*, 759, L43
 Chomiak, D., Taleb-Bendiab, A., Civiš, S., & Amano, T. 1994, *Can. J. Phys.*, 72, 1078
 Dore, L., Cazzoli, G., Civiš, S., & Scappini, F. 1995, *Chem. Phys. Lett.*, 244, 145
 Flower, D. R., Pineau Des Forêts, G., & Walmsley, C. M. 2005, *A&A*, 436, 933
 Flower, D. R., Pineau Des Forêts, G., & Walmsley, C. M. 2006, *A&A*, 449, 621
 Garrod, R. T., & Herbst, E. 2006, *A&A*, 457, 927
 Geppert, W. D., Hamberg, M., Thomas, R. D., et al. 2006, *Faraday Discuss.*, 133, 177
 Gerin, M., Goicoechea, J. R., Pety, J., & Hily-Blant, P. 2009, *A&A*, 494, 977
 Gómez Martín, J., Caravan, R., Blitz, M., Heard, D., & Plane, J. 2014, *J. Phys. Chem. A*, 118, 2693
 Guzmán, A., Pety, J., Goicoechea, J. R., Gerin, M., & Roueff, E. 2011, *A&A*, 534, A49
 Hamberg, M., Geppert, W. D., Thomas, R. D., et al. 2007, *Mol. Phys.*, 105, 899
 Jiménez, E., Antíñolo, M., Ballesteros, B., Canosa, A., & Albaladejo, J. 2016, *Phys. Chem. Chem. Phys.*, 18, 2183
 Le Gal, R., Hily-Blant, P., Faure, A., et al. 2014, *A&A*, 562, A83
 McElroy, D., Walsh, C., Markwick, A. J., et al. 2013, *A&A*, 550, A36
 Minh, Y. C., Irvine, W. M., & McGonagle, D. 1993, *J. Kor. Astron. Soc.*, 26, 99
 Müller, H. S. P., Thorwirth, S., Roth, D. A., & Winnewisser, G. 2001, *A&A*, 370, L49
 Müller, H. S. P., Schlöder, F., Stutzki, J., & Winnewisser, G. 2005, *J. Mol. Struct.*, 742, 215
 Ohishi, M., Ishikawa, S.-I., Amano, T., et al. 1996, *ApJ*, 471, L61
 Osborne, Jr., D. S., Lawson, P. A., & Adams, N. G. 2015, *Int. J. Mass Spectr.*, 378, 193
 Pirim, C., & Krim, L. 2011, *Chem. Phys.*, 380, 67
 Prasad, S. S., & Huntress, Jr., W. T. 1980, *ApJS*, 43, 1
 Roy, A., André, P., Palmeirim, P., et al. 2014, *A&A*, 562, A138
 Shannon, R. J., Blitz, M. A., Goddard, A., & Heard, D. E. 2013, *Nature Chem.*, 5, 745
 Vastel, C., Ceccarelli, C., Lefloch, B., & Bachiller, R. 2014, *ApJ*, 795, L2
 Vasyunin, A. I., & Herbst, E. 2013, *ApJ*, 769, 34
 Wakelam, V., Herbst, E., Loison, J.-C., et al. 2012, *ApJS*, 199, 21